

Metal-insulator transition in three-dimensional Anderson superlattice with rough interfacesSomaye Jafari,¹ Ameneh Sheikhan,² Ayoub Esmailpour,^{3,4} Mehraz Anvari,⁵ and M. Reza Rahimi Tabar^{5,6}¹*Institute for Nanoscience and Nanotechnology (INST), Sharif University of Technology, P.O. Box 14588-89694, Tehran, Iran*²*National Institute for Theoretical Physics, Private Bag XI, 7602 Matieland, South Africa*³*Department of physics, Shahid Rajaei Teacher Training University, Lavizan, Tehran 16788-15811, Iran*⁴*School of Physics, Institute for Research in Fundamental Sciences, IPM, 19395-5531 Tehran, Iran*⁵*Department of Physics, Sharif University of Technology, 11365-9161 Tehran, Iran*⁶*Institute of Physics, Carl-von-Ossietzky, University Oldenburg, D - 26111 Oldenburg, Germany*

(Received 26 February 2012; revised manuscript received 21 April 2012; published 18 June 2012)

We study the electronic properties of superlattice with rough interfaces in two and three dimensions using the transfer-matrix method and direct diagonalization of the Anderson Hamiltonian. The system consists of layers with an average constant width, but with stochastic roughness added to the interfaces between the layers. The numerical results indicate that, in the thermodynamic limit, the two-dimensional superlattice is an insulator in the presence of even small roughness. In three-dimensional systems, however, the superlattice exhibits a metal-insulator transition with a well-defined mobility edge located at an energy E_c that we compute numerically. For three-dimensional superlattice, the localization length follows a power law near the mobility edge $\xi(E) \sim (E_c - E)^{-\nu}$, where the exponent is $\nu \simeq 1.6$. We also show that the existence of the extended states in three-dimensional superlattices gives rise to a finite conductivity in the limit $M/L \rightarrow \infty$, where L is the length and M the width of the bar.

DOI: [10.1103/PhysRevB.85.224204](https://doi.org/10.1103/PhysRevB.85.224204)

PACS number(s): 71.30.+h, 72.15.Rn, 68.35.Ct

An important problem in the fabrication of electronic and optical instruments is the existence of interface roughness. The roughness limits the efficiency of optoelectronic devices, and it is essential for the functionality of the quantum wells and the superlattices. The theory of electron and wave scattering from rough interfaces has been developed in Refs. 1 and 2. The influence of interface roughness on electronic transport properties has been studied extensively in GaAs/AlGaAs heterostructures,³⁻⁷ where the validity of the theory has been confirmed.

A thorough understanding of the nature of heterointerfaces is essential to correlating interface roughness with the optoelectronic properties of complex systems, such as superlattices whose structures are composed of alternating layers of two or more materials arranged either randomly or periodically.⁸ They are of interest due to their applications in such devices as semiconductor lasers,^{9,10} optical data-storage media,¹¹ thermoelectric systems,¹²⁻¹⁵ thermomechanic systems,¹⁶ microelectronic systems,¹⁷ graphene,¹⁸ composite films,¹⁹ etc.

Electronic properties of multilayered semiconductor superlattices have been investigated by many researchers over the past decades. Esaki and Tsu²⁰ proposed the concept of semiconducting superlattices, and they suggested the possibility of obtaining experimental evidence of Bloch oscillations in a superlattice structure. In electronic transport studies of superlattices, it is usually assumed that the system is structurally perfect. When a superlattice is grown, however, due to the random nature of the growth techniques, disorder such as interface roughness is generated in the system.²¹ It is also known that interfacial roughness plays an important role in the thermal conductivity of superlattices.²²⁻²⁷

Here, we focus on the role of interfacial roughness on the electronic properties of superlattices. Using the transfer-matrix (TM) method and direct diagonalization of the Hamiltonian, we show that interface roughness greatly influences electronic transport in two-dimensional (2D) and 3D superlattices. Our

numerical results indicate that, in the thermodynamic limit, the 2D system is an insulator in the presence of even small interfacial roughness. In 3D systems, however, the superlattice exhibits a metal-insulator transition with a well-defined mobility edge that our simulations identify at the energy $E_c \simeq \pm 4.9$. We also show that the existence of extended states in 3D superlattices with rough interfaces gives rise to a finite dc conductivity in the limit $M/L \rightarrow \infty$.

Let us start with the Anderson model for 2D systems. We use the nearest-neighbor tight-binding model, defined by

$$\psi_{n+1,m} + \psi_{n-1,m} + \psi_{n,m+1} + \psi_{n,m-1} = (E - \epsilon_{n,m})\psi_{n,m} \cdot x \quad (1)$$

Equation (1), which is extended to 3D systems straightforwardly, is the discrete version of the model defined by $H\psi = \epsilon\psi$, where $E = 4 - \frac{2ma^2}{\hbar^2}\epsilon$ is the shifted energy and ϵ is the eigenvalue of the Hamiltonian. The function $\psi_{n,m}$ denotes the amplitude of the wave function at site (m,n) of the lattice with a lattice constant a , which we set to be unity. We then consider a multilayered or superlattice structure with rough interfaces between the layers. The geometry of the 2D superlattice is shown in Fig. 1. It consists of two kinds of alloys, say A and B . There are two on-site energies in any layer, namely $\epsilon_{n,m} = \epsilon_A$ or $\epsilon_{n,m} = \epsilon_B$. We set $\epsilon_A = 1$ and $\epsilon_B = -1$.

The ordered superlattice without interface roughness is transparent. In practice, however, the surface between materials A and B is not flat but rough. To model the rough interfaces in, for example, 2D superlattices, we use a white noise disorder to generate the roughness at the interfaces between the layers. The width of each layer in the superlattice, such as, for example, in the x direction (horizontal direction in the figure), is W . In each layer we add a randomly selected value $\delta(x,y)$ to the average position of the n th layer, i.e., $x(n,y) = nW + \delta(x,y)$, where $\delta(x,y)$ is a random and uncorrelated stochastic variable with zero mean, distributed uniformly in the interval $[-\sigma, \sigma]$. This means that if the on-site

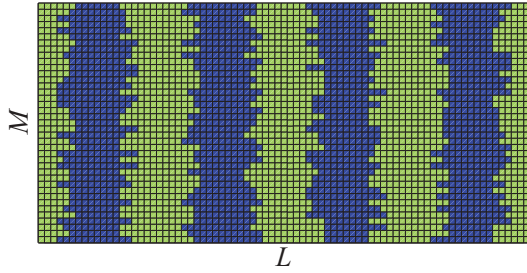


FIG. 1. (Color online) The geometry of a superlattice in 2D. Different colors relate to a different medium in the superlattice. The average width of each layer in the superlattice is W . In each layer we add a randomly selected value $\delta(x, y)$ to the average position of the n th layer, i.e., $x(n, y) = nW + \delta(x, y)$, where $\delta(x, y)$ is a random and uncorrelated (white noise) stochastic variable with zero mean, distributed uniformly in the interval $[-\sigma, \sigma]$. The on-site energy in the n th layer is $\epsilon_A = 1$, and in the $(n + 1)$ st layer it will be $\epsilon_B = -1$.

energy in the n th layer is ϵ_A , then the on-site energy in the $(n + 1)$ st layer will be ϵ_B . Adding randomness at the interface between layers with ϵ_A and ϵ_B causes the penetration of two regions into each other, as shown in Fig. 1. Hence, the disorder in the superlattice, which is the roughness of the interfaces between the layers, is generated by the stochastic variable $\delta(x, y)$ with its strength controlled by σ .

Numerical simulations were carried out for 2D strips as well as 3D bars. Using the TM method, we computed the smallest positive Lyapunov exponent γ , the inverse of the localization length. Equation (1) is rewritten as a recursive equation,

$$\begin{pmatrix} \Psi_{k+1} \\ \Psi_k \end{pmatrix} = \begin{pmatrix} EI - H_k & -I \\ I & 0 \end{pmatrix} \begin{pmatrix} \Psi_k \\ \Psi_{k-1} \end{pmatrix} = T_k \begin{pmatrix} \Psi_k \\ \Psi_{k-1} \end{pmatrix}, \quad (2)$$

where T_k is the TM for the k th layer and Ψ_k is the vector that contains the values of ψ in T_k , and so on. The rough superlattice is represented by an $M \times L$ strip in 2D and an $M \times M \times L$ bar in 3D, with periodic boundary conditions, where M is the width and L is the longitudinal length. Every element in the TM is a $2M \times 2M$ matrix in 2D and a $4M^2 \times 4M^2$ matrix in 3D. The H_k is the sub-Hamiltonian of the k th part. By specifying the initial values of Ψ in the first and second lines of the strip in 2D and the first and second planes of the bar in 3D, we compute the amplitude of the wave function at length L by multiplying all of the TMs.

The Lyapunov exponents are the logarithm of the eigenvalues of the matrix $(\mathbf{T}\mathbf{T}^t)^{1/2L}$, where t denotes the transpose operation, and $\mathbf{T} = \prod_{k=1}^L \mathbf{T}_k$.²⁸ Using the TM, we computed the smallest positive Lyapunov exponent γ , which represents the inverse of the localization length. The Lyapunov exponent is a measure to describe the localization properties of the disordered systems. It characterizes the exponential decay of the wave function, satisfies a multiplicative central limit theorem, and approaches a nonrandom value, γ , when the size of the system tends to infinity.²⁹ The localization length $\xi(E)$ of a state with a given energy E is related to γ as $\xi(E) = \gamma^{-1}$.

The number of the Lyapunov exponents is $N = 2M$ for 2D systems and $N = 4M^2$ for 3D superlattices. The simulations begin by N orthogonal initial vectors, followed by the Gram-Schmidt (GS) orthogonalization after every four steps of the

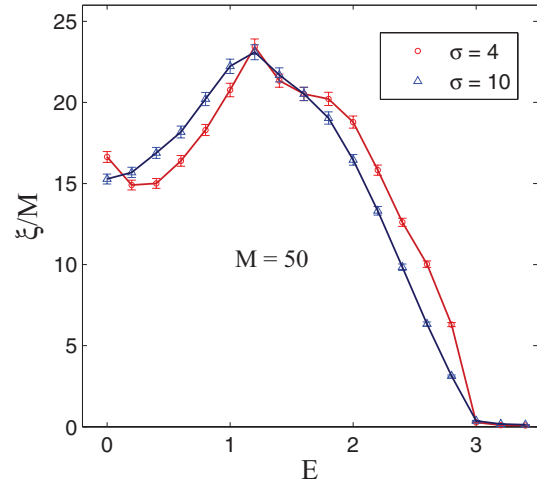


FIG. 2. (Color online) Rescaled localization length of a two-dimensional superlattice as a function of energy for two values of the strength of roughness.

TM iteration. The reason for the use of the GS orthogonalization is that, after some iterations, the directions of all the vectors change to the direction of the vector that corresponds to the *largest* Lyapunov exponent. Use of orthogonalization enables us to determine the smaller Lyapunov exponents, particularly the smallest one. The iterations are continued until an acceptable relative accuracy is achieved for the rescaled localization length, $\Lambda = \xi/M$. Finite-size scaling of Λ identifies the localized and delocalized states. Increasing the width of the strip or the bar affects the behavior of Λ for different energies.

For given energy and the strength of roughness, Λ either increases, indicating that the state is delocalized, or decreases, implying that the state is localized. Therefore, using such properties of the rescaled localization length, we distinguish the extended states from the localized ones, as well as the metal system from the insulator regime.

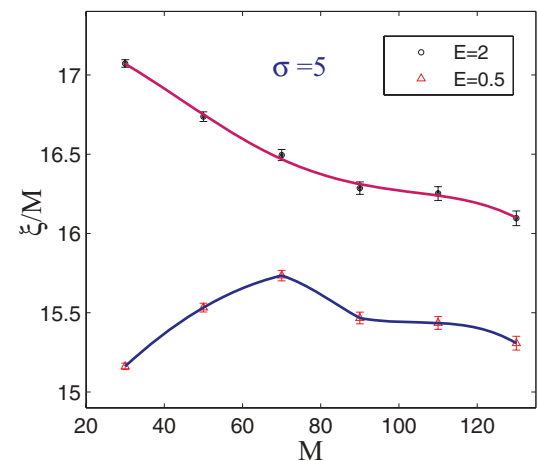


FIG. 3. (Color online) Variation of the rescaled localization length with respect to the width of the system M for two energies and for a superlattice with the roughness strength $\sigma = 5$ in two dimensions.

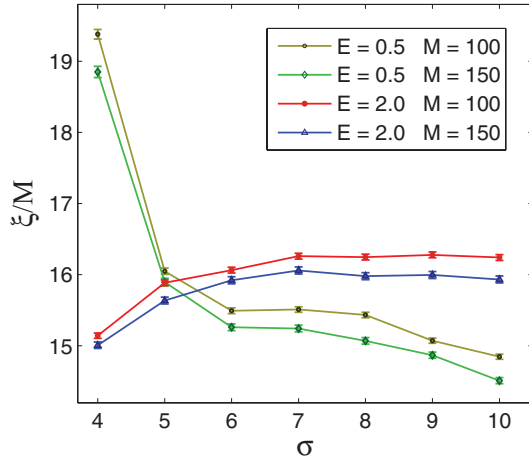


FIG. 4. (Color online) Rescaled localization length as a function of the strength of roughness for two values of energies and for two widths M in a two-dimensional superlattice.

Let us now present the numerical results. Using direct diagonalization, we estimated the allowed energies of the system, which are needed in the TM method in order to calculate the localization length. We found that the energy interval belongs to $-5 \lesssim E \lesssim 5$ in the 2D system and to the interval $-6 \lesssim E \lesssim 6$ in the 3D superlattice. For a 2D superlattice with flat interfaces, the energy interval is in $[-4, 4]$.

We then calculated the localization length ξ as a function of energy E in the presence of roughness at the interfaces between the layers. Figure 2 presents the rescaled localization length ξ/M in 2D in terms of the energy E for two values of the strength of roughness, $\sigma = 4$ and 10. The width of the strip is $M = 50$, while the width of each layer is $W = 16$. Figure 2 is plotted only for energies in the range $(0, 5)$, but the results are similar in the range $(-5, 0)$.

Figure 3 depicts the dependence of the rescaled localization length on the width M of the strip for two energies, $E = 2$ and 0.5, in two dimensions. The rescaled localization length decreases by increasing the width of the bar, indicating that the

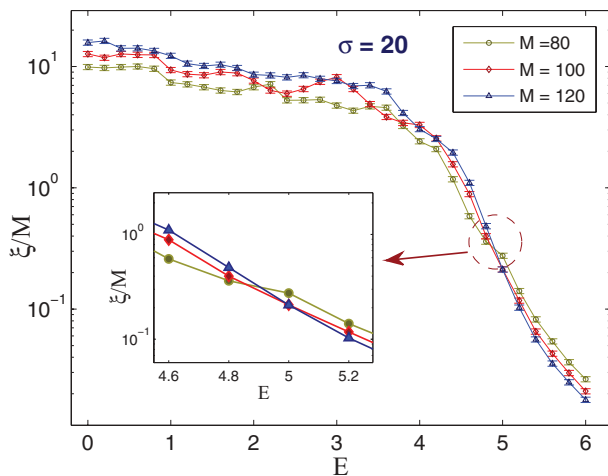


FIG. 5. (Color online) Rescaled localization length of a three-dimensional superlattice as a function of energy for two widths M and for the strength of roughness $\sigma = 20$.

two energies are localized. Here, the strength of the roughness is $\sigma = 4$ and the width of each layer is $W = 16$. Then, for fixed energy E and width M , we varied the strength σ of the roughness. Figure 4 depicts the dependence of the rescaled localization length on the strength of roughness for several energies and widths of the 2D strip. These results indicate that the localization length does not decrease if the strength of the roughness increases for some energies. However, for both energies $E = 2$ and 0.5 and for all roughness strengths σ , the rescaled localization length decreases by increasing the width of the strip, which is consistent with the results of Fig. 3. We conclude as a result that the 2D superlattices are an insulator in the presence of even very small white noise in the interface's roughness. This is one of the main results of this paper.

We now present the numerical results for a 3D superlattice. Figure 5 shows the rescaled localization length versus energy for various widths of the bar for a roughness strength of $\sigma = 20$, when the width of each layer is $W = 50$. In this case,

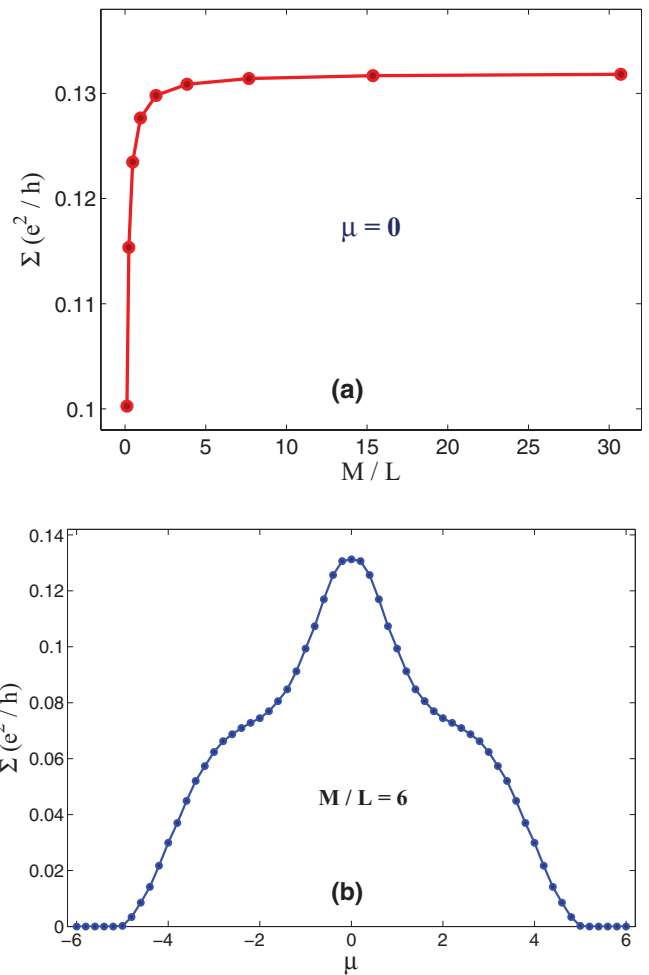


FIG. 6. (Color online) (a) Conductivity as a function of the aspect ratio of the system for a vanishing chemical potential μ . The thermodynamic limit is defined as $M/L \rightarrow \infty$. We note that this limit is reached for moderate aspect ratios $M/L \geq 6$. The dc conductivity is given for the strength of disorder $\sigma = 20$. The conductivity approaches $\simeq 0.13(e^2/h)$ in the thermodynamic limit. (b) The μ dependence of the conductivity for a fixed aspect ratio $M/L = 6$.

there exist two different behaviors for Λ when the width M of the bar increases. For low energies, Λ increases, which is related to the delocalized states, whereas for high energies the rescaled localization length decreases, indicating that the states are localized. The energy $E_c \approx 4.9$ represents the mobility edge, which is scale-invariant and is the critical energy. Thus, the rescaled localization length undergoes a phase transition in the presence of roughness in a 3D superlattice with rough interfaces. The inset of the figure presents the behavior of the rescaled localization length close to the critical energy, proving the existence of the metal-insulator transition in 3D superlattices with rough interfaces. Using the method used in Ref. 30, one can show that for a three-dimensional superlattice, the localization length follows a power law near the mobility edge $\xi(E) \sim (E_c - E)^{-\nu}$, where E_c is the critical energy. We find the scaling exponent to be $\nu = 1.60 \pm 0.05$. We note that the estimated critical exponent is the same as that of the 3D Anderson model with random binary disorder³¹ and it is also close to $\nu = 3/2$, which was recently derived based on a semiclassical theory for the 3D Anderson model of electron localization.³²

Having calculated the localization length, we computed the dc conductivity of the superlattice in 3D and determined its dependence on the chemical potential μ .^{33,34} The conductivity

$\Sigma = G \times L/M^2$ as a function of the aspect ratio of the system (at 300 K) is given in Fig. 6(a) for a vanishing chemical potential μ . The conductance G was calculated using the Engquist-Anderson relation.³³ Here, the thermodynamic limit is defined by the limit $M/L \rightarrow \infty$.³⁵ We note that this limit is already reached for moderate aspect ratios, $M/L \geq 6$. The dc conductivity is given for the strength of disorder, $\sigma = 20$. It approaches $\simeq 0.13(e^2/h)$ in the thermodynamic limit. In Fig. 6(b), we plot the μ dependence of the conductivity for a fixed aspect ratio $M/L = 6$. The conductivity has a maximum in the limit $\mu = 0$.

In summary, we studied 2D and 3D superlattices with rough interfaces. We showed that 2D superlattices are localized for any strength of roughness. It was shown by increasing the strength of roughness that the localization length may increase or decrease, depending on the energy E . In the thermodynamic limit, however, the system will be an insulator. We proved that there exists a metal-insulator transition in 3D superlattices with rough interfaces, and we determined the mobility-edge energy. For three-dimensional superlattices with rough interfaces, the critical exponent that characterizes the power-law behavior of the localization length near the transition point is about $\nu \simeq 1.6$. We also computed the dc conductance of a 3D superlattice and its variations with the chemical potential.

¹R. E. Prange and T. W. Nee, *Phys. Rev.* **168**, 779 (1968).

²A. Gold, *Phys. Rev. B* **35**, 723 (1987).

³H. Sakaki, T. Noda, K. Hirakawa, M. Tanaka, and T. Matsusue, *Appl. Phys. Lett.* **51**, 1934 (1987).

⁴R. Göttinger, A. Gold, G. Abstreiter, G. Weimann, and W. Schlapp, *Europhys. Lett.* **6**, 183 (1988).

⁵U. Bockelmann, G. Abstreiter, G. Weimann, and W. Schlapp, *Phys. Rev. B* **41**, 7864 (1990).

⁶V. A. Kulbachinskii, V. G. Kytin, A. I. Kadushkin, E. L. Shangina, and A. de Visser, *J. Appl. Phys.* **75**, 2081 (1993).

⁷B. Yang, Y.-h. Cheng, Z.-g. Wang, J.-b. Liang, Q.-w. Liao, L.-y. Lin, Z.-p. Rough Zhu, B. Xu, and W. Li, *Appl. Phys. Lett.* **65**, 3329 (1994).

⁸G. D. Mahan, *Thermal Conductivity of Superlattices*, in *Thermal Conductivity: Theory, Properties, and Applications (Physics of Solids and Liquids)*, edited by T. M. Tritt (Kluwer Academic/Plenum Publishers, New York, 2004).

⁹T. E. Sale, *Cavity and Reflector Design for Vertical Cavity Surface Emitting Lasers* (Institution of Electrical Engineers, Stevenage, UK, 1995).

¹⁰J. Faist, F. Capasso, D. L. Sivco, C. Sirtori, A. L. Hutchinson, and A. Y. Cho, *Science* **264**, 553 (1994).

¹¹E. K. Kim, S. I. Kwun, S. M. Lee, H. Seo, and J. G. Yoon, *Appl. Phys. Lett.* **76**, 3864 (2000).

¹²L. D. Hicks, T. C. Harman, and M. S. Dresselhaus, *Appl. Phys. Lett.* **63**, 3230 (1993).

¹³Y.-M. Lin, O. Rabin, S. B. Cronin, J. Y. Ying, and M. S. Dresselhaus, *Appl. Phys. Lett.* **8**, 2403 (2002); Y.-M. Lin and M. S. Dresselhaus, *Phys. Rev. B* **68**, 075304 (2003).

¹⁴R. Venkatasubramanian, E. Siivola, T. Colpitts, and B. O'Quinn, *Nature (London)* **413**, 597 (2001).

¹⁵T. C. Harman, P. J. Taylor, M. P. Walsh, and B. E. LaForge, *Science* **297**, 2229 (2002).

¹⁶Y. Ezzahri, G. Zeng, K. Fukutani, Z. Bian, and A. Shakouri, *Microelectron. J.* **39**, 981 (2008).

¹⁷Y. Huang, X. Duan, Y. Cui, L. J. Lauhon, K.-H. Kim, and C. M. Lieber, *Science* **294**, 1313 (2001).

¹⁸N. Abedpour, A. Esmailpour, R. Asgari, and M. R. Tabar, *Phys. Rev. B* **79**, 165412 (2009).

¹⁹E. N. Oskoe and M. Sahimi, *Phys. Rev. B* **74**, 045413 (2006).

²⁰L. Esaki and R. Tsu, *IBM J. Res. Dev.* **14**, 61 (1970).

²¹I. Dharssi and P. N. Butcher, *J. Phys.: Condens. Matter* **2**, 4629 (1990).

²²G. Chen, *Phys. Rev. B* **57**, 14958 (1998).

²³B. C. Daly, H. J. Maris, K. Imamura, and S. Tamura, *Phys. Rev. B* **66**, 024301 (2002); R. Venkatasubramanian, *ibid.* **61**, 3091 (2000); T. Kawamura, Y. Kangawa, and K. Kakimoto, *J. Cryst. Growth* **298**, 251 (2007).

²⁴B. C. Daly and H. J. Maris, *Physica B* **316–317**, 247 (2002).

²⁵Y. Chen, D. Li, J. R. Lukes, Z. Ni, and M. Chen, *Phys. Rev. B* **72**, 174302 (2005).

²⁶G. Chen, *ASME J. Heat Transfer* **119**, 220 (1997).

²⁷B. C. Daly, H. J. Maris, Y. Tanaka, and S. Tamura, *Phys. Rev. B* **67**, 033308 (2003).

²⁸A. MacKinnon and B. Kramer, *Rep. Prog. Phys.* **56**, 1469 (1993).

²⁹V. I. Oseledets, Trudy. Moskov. Mat. Obshch. **47**, 179 (1968).

- ³⁰A. Sheikhan, M. R. Tabar, and M. Sahimi, *Phys. Rev. B* **80**, 035130 (2009); R. Sepehrinia, M. R. RahimiTabar, and M. Sahimi, *ibid.* **78**, 024207 (2008); F. Shahbazi, A. Bahraminasab, S. M. VaezAllaei, M. Sahimi, and M. R. Tabar, *Phys. Rev. Lett.* **94**, 165505 (2005).
- ³¹I. V. Plyushchay, R. A. Romer, and M. Schreiber, *Phys. Rev. B* **68**, 064201 (2003).
- ³²A. M. Garcia-Garcia, *Phys. Rev. Lett.* **100**, 076404 (2008).
- ³³H. L. Engquist and P. W. Anderson, *Phys. Rev. B* **24**, 1151 (1981).
- ³⁴A. Esmailpour, M. Esmailzadeh, E. Faizabadi, P. Carpena, and M. R. Tabar, *Phys. Rev. B* **74**, 024206 (2006); A. Esmailpour, M. Esmailpour, A. Sheikhan, M. Elahi, M. R. Tabar, and M. Sahimi, *ibid.* **78**, 134206 (2008).
- ³⁵J. Tworzydło, B. Trauzettel, M. Titov, A. Rycerz, and C. W. J. Beenakker, *Phys. Rev. Lett.* **96**, 246802 (2006).